Comparative Study of Motor Topologies for Electric Power Steering System

H. Yang[1], S. Ademi[1*], J. Paredes[2] and R. A. McMahon[1]
[1]*WMG, University of Warwick,* Coventry, UK
[2]*Transport & Energy Division of CEIT and University of Navarra,* Spain
*s.ademi@warwick.ac.uk

Abstract—**Electric power steering (EPS) plays a critical role towards safety and comfort especially for modern vehicles with ever-increasing complexity. The evolution of EPS technologies require not only vehicle dynamics and fuel efficiency but also higher standards of steering function. Apart from providing essential electromechanical energy conversion, the performance of EPS motor has received attention from industry and academic community in terms of high torque/power density and low level of noise and vibration. This paper details aspects of design and analysis of permanent magnet synchronous motor (PMSM) for EPS application. Furthermore, the concept of multi-phase motor is adopted factoring redundancy design in achieving fail-operational for safety critical applications such as steer-by-wire (SbW) system for autonomous driving. The motor topologies investigated have been modelled utilising Motor-CAD software.**

Keywords— Permanent magnet synchronous motor, electric power steering, multi-phase motor, steer-by-wire, fail-operational.

I. INTRODUCTION

Power assisted steering is very widely used in modern road vehicles. The earliest implementation was hydraulic power steering (HPS), followed by electric-hydraulic power steering (EHPS), then electric power steering (EPS), as depicted in Fig. 1, and most recently steer-by-wire (SbW) systems. The continuing development to these systems has not only resulted in improved steering functionality, such as assisted parking handling stability, but also increased energy efficiency [1].
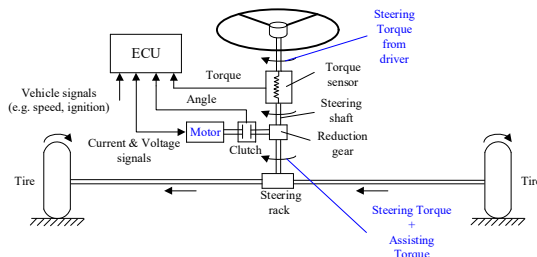

Fig. 1. Architecture of a column-type EPS system [1].

As the key actuators in an EPS system, the electric motor converts electric energy to the mechanical energy demanded during steering. The requirements for the electric motor in an EPS system are similar to servo motor applications, which require high torque/power density while at the same time encompassing compact size, low rotor inertia, low torque ripple and fault tolerance. Moreover, safety requirements demand that steering functionality moves from fail-safe to fail-operational for highly automated systems such as the SbW configuration. Various motor types have been employed in EPS systems, mainly driven by power requirement demands [2]. Contemporary EPS systems use AC motors, including induction motors (IMs) and permanent magnet synchronous motors (PMSMs). IMs have been investigated due to its robustness and PM-free characteristics for medium-power EPS application [3]. Yet, a comparison of the performance between six-phase IMs and PMSMs on the basis of identical inverter currents, showed that the PMSM provides a 10% larger output torque density than the IM counterpart [4]. PMSMs, including surface-mounted permanent magnet (SPMs) motors and interior permanent magnet (IPMs) motors, have therefore been the motor of choice for mid-size and luxury cars, giving increased power density and efficiency [5]. Further, research on the topic has focused on improving the feel of the steering from the viewpoint of mitigating cogging torque [6] and torque ripple reduction [7]. Reluctance motors, i.e. switched reluctance motor (SRM) and synchronous reluctance motor (SynRel), have also been considered as options for EPS application, taking advantage of their mechanical and thermal robustness [8], [9].

Achieving an acceptable level of safety is challenging in SbW structure, as there is no mechanical linkage between the steering wheel and steering mechanism. The challenge is especially great in autonomous driving, especially at level 5. Multi-phase machines have emerged as candidates for achieving fail-operational in an event of faults [10-12]. Dual three-phase EPS systems equipped with IM and SRM have been investigated to improve fault-tolerance in an EPS system [4], [13]. Ref. [10] offers a 2-drive motor control solution with dual three-phase IPM, which delivers 50% torque output in a failure state whilst claiming a 30% reduction in size and 20% reduction in weight compared to its previous EPS systems. This paper describes the analysis and design of a dual three-phase motor in order to achieve the fault tolerance capability of an EPS system. However, the fail-safe analysis of the dual three-phase IPM is out of the scope in this work.

Section II presents a systematic review in selecting an appropriate motor topology for a given EPS application and introduces various requirements for power steering systems. The electromagnetic performance of two PMSMs intended for a rack-type EPS system are detailed in section III. The improved fault tolerance and torque ripple reduction of the PM motors are given in section IV. General conclusions are provided in section V.

II. TRENDS IN POWER STEERING SYSTEMS

Manual steering with control by a steering wheel has been around since 1898 [14]. Steering assistance has continuously evolved over the years, and in doing so various demands have been identified to overcome the increasing difficulties in turning the steering wheel as vehicle weights and hence wheel loads have become higher. HPS was increasingly deployed from the 1950s onwards to reduce steering effort in passenger cars. In a conventional HPS system (Fig. 2), the drivers steering torque is multiplied by a series of components in the hydraulic unit including a hydraulic piston and a steering pump [15]. HPS systems have the advantage since they provide a pleasant steering feel between the driver and the

road they operate independently from the vehicles electrical system. However, in such systems the pump presents an active load to the engine no matter if the steering is required or not, which increases fuel consumption.
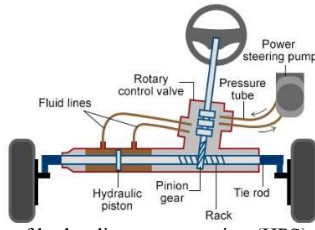

Fig. 2. An overview of hydraulic power steering (HPS).

With an increased focus on fuel economy after the energy crisis in 1970s, an electric motor was used for the power steering pump giving rise to electric hydraulic power steering (EHPS). In an EHPS system (Fig. 3), hydraulic pump is separated from the engine and driven directly by an electric motor, giving increased flexibility in system layout. Nevertheless, EHPS still has the drawbacks of requiring a hydraulic system [16].
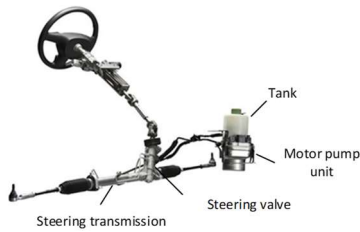

Fig. 3. Representation of an electric hydraulic power steering (EHPS).

With the invention of EPS in the late 1980s, steering assistance was fully achieved by an electric motor. The EPS system brought a sizeable weight reduction (more than 3.5 kg) in comparison to HPS reflecting the removal of the mechanical components starting with belts, pulleys, pump, oil tank and hydraulic lines. The complexity of the steering system has progressively reduced leading to the column-type EPS system, for example manufactured by JTEK Corp, as depicted in Fig. 4 [17]. One of the major advantages offered by the EPS (Fig. 4) is the significant reduction in carbon dioxide emissions due to fuel saving [1]. It also reiterates that the EPS in large vehicles can improve 15% fuel economy compared to the conventional HPS as EPS motor is only active when the steering wheel is being manoeuvred by the driver.

Fig. 4. Simplified electric power steering (EPS).

Furthermore, steering operation has been improved thanks to the integration of technologies including motor, sensors and electronic control unit (ECU). Online steering force regulation can be achieved by control algorithms in the ECU according to speed and load demands. The steering characteristics of an EPS can be easily programmed and adjusted to suit different vehicle types. Although EPS systems have great design flexibility as summarised in Table I. The selection of most appropriate motor topology should be carefully considered against a given vehicle specification.

TABLE I.   TYPICAL EPS SYSTEMS AND MOTOR REQUIREMENTS

EPS type	Column type (C-EPS)	Pinion type (P-EPS)	Rack type (R-EPS)
System configuration			
Motor location	On steering column	Underhood area	Connected to the rack
Application	Small-size vehicles	Medium-size vehicles	Large-size vehicles
Rack force (kN)	6 – 8	7 – 12	9 – 16
Motor output power (kW)	0.2 – 0.7	0.5 – 0.7	0.4 – 1.2
Motor torque (N·m)	Small	Intermediate	Large
Noise and vibration	Low (motor is close to the driver)	Less required than C-EPS	Low
Package requirement	Less required	Highly required for smaller size and light weight	Highly required in liquid and thermal endurance

Despite the relative maturity of EPS systems, failures have been reported which have led to a sudden loss of power assistance while driving [18]. An electronic failure in the conventional EPS system simply leads to fail-safe mode, which falls back to manual steering albeit with heavy manual turning effort. Hence, the reliability of EPS must be improved further in order to achieve fail-operational in the event of a fault, essential in SbW architectures. A system, which includes two independent motors, power electronic circuitry and power supply, can provide 50% of normal steering assistance in the event of system failure; such an arrangement is illustrated in Fig. 5 [19]. The development and increasing use of SbW, along with the rise of autonomous driving, mandates a redundant architecture for the steering function. Such systems entail of the following advantages over conventional EPS systems:

- Simplification of manufacturing processes and vehicle assembly;
- More space freedom in packaging arising from the elimination of mechanical steering column;
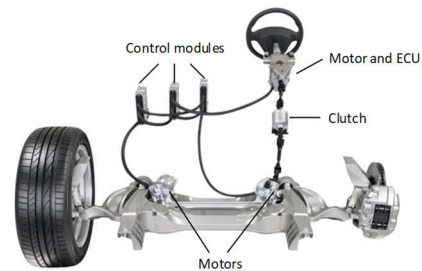- Improved steering functionality with increased safety and reliability in driving.

Fig. 5. Steer-by-wire created by Nissan/Infiniti.

The trend in steering systems can be summarised as continuous progress, with mechanical components being progressively replaced by electrical ones.

III. COMPARATIVE STUDY OF MOTOR TOPOLOGIES FOR AN ELECTRIC POWER STEERING SYSTEM

Based on the aforementioned review of different steering systems, this section focuses on the design and analysis of two different permanent magnet synchronous motors, i.e., SPM and IPM motors, for a specific rack-type EPS application, which demands high output torque and power in a compact size. The specification of this EPS motor in terms of the space envelope and electrical requirements are tabulated in Table II.

TABLE II. CONSTRAINS ON EPS MOTOR SPECIFICATION

Parameter	Symbol	Unit	Value
Stator outer diameter	D_{os}	mm	90
Lamination active length	L_a	mm	90
DC link voltage	U_{dc}	V	48
Excitation current	I_{rms}	A	30
Rated power for EPS motor	P_{out}	W	820
Base speed	ω_n	rpm	1650
PM remanence @ 20°C	B_r	T	1.35
PM relative permeability	μ_r	-	1.05
Air-gap length	g	mm	1.0
Packing factor	k_p	-	0.4
Cooling method	Totally-Enclosed Non-Ventilated (TENV)		

SPM and IPM motors have been modelled utilising Motor-CAD, as illustrated in Fig. 6. Both designs consist of identical stator/rotor pole number combination, i.e., 12 stator-slot/10 rotor-pole (12s/10p) and same concentrated non-overlapping winding topology. Therefore, the corresponding phase vectors and winding arrangement for both motor topologies are depicted in Fig. 7. Since there are two coil sides in one stator slot, such type of winding arrangement is referred to as a double-layer (DL) winding [20]. The major difference between the two motor topologies investigated is the rotor configurations. For the SPM motor, the PMs are retained and glued on the rotor surface, whereas for the IPM motor, the PMs are buried inside the rotor. The relative electromagnetic performance of the two motors have be investigated in the following sub-sections.
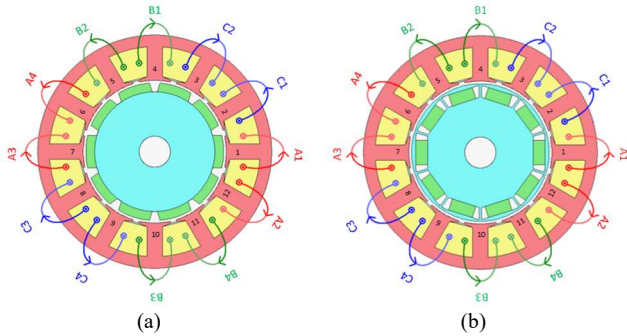

Fig. 6. Radial cross sections of the dual three-phase 12s/10p PMSMs with double layer winding. (a) SPM motor and (b) IPM motor.
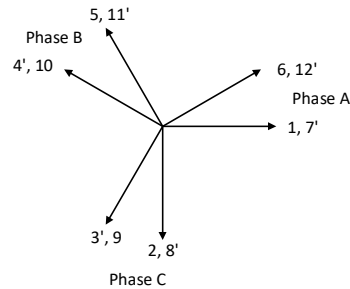

Fig. 7. Phase vectors for the dual three-phase 12s/10p PMSMs with double layer winding.

A. Open-circuit back-EMF and cogging torque

When rotors of the two motors are rotating at the same speed, the back-EMF waveforms induced in the armature windings are as illustrated in Fig. 8(a). Results show that fundamental component of the SPM is 55.9% higher than the IPM, attributable to the higher air-gap flux density. Based on the Fig. 8(b), a higher amplitude of the 3rd harmonic is observed in the spectrum of the SPM while higher order harmonics are negligible in the IPM. The cogging torque is intrinsic to PM motors due to the interaction between the stator and rotor. The waveforms and spectrum of the cogging torque for the two motors are depicted in Fig. 9. The SPM has a much higher peak value of cogging torque compared to the IPM, which is a major issue for an EPS system. Some techniques, such as skewing, stepping and air-gap shaping, are commonly applied to mitigate cogging torque in order to provide smooth steering feel to the driver [6], [21], [22].
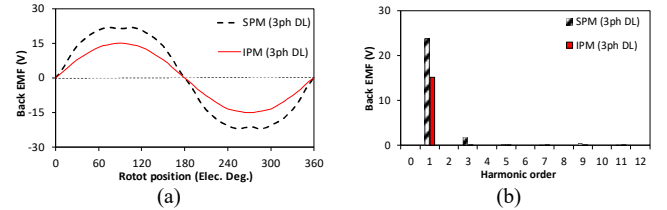

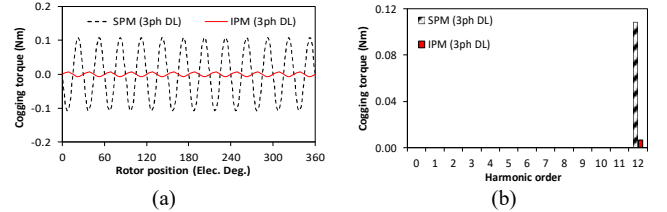Fig. 8. OC back-EMF at 1650 rpm. (a) Waveforms and (b) Spectrum.

Fig. 9. Cogging torque. (a) Waveforms and (b) Spectrum.

B. Healthy and faulty performance operating conditions

Under healthy operation conditions, balanced three-phase currents are fed into armature windings and on-load shaft torque is generated (Fig. 10). The SPM has 54.9% higher average torque than the IPM thanks to the higher fundamental component of the back-EMF. Torque ripple, which is defined as the ratio of the peak-to-peak fluctuation to the average torque value, of the SPM and the IPM is 5.8% and 3.7% at the rated current. Since the PMs are located on the rotor, the PMs serve as the constant excitation source. This inherent characteristic of PMSM can be a safety risk in a fault condition, especially if a short-circuit (SC) fault occurs in the winding.
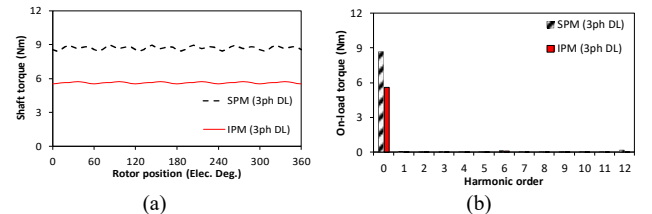

Fig. 10. On-load torque performance of the dual three-phase 12s/10p PMSMs at I_{rms} = 30 A. (a) Waveforms and (b) Spectrum.

The likelihood of SC fault in electrical machines has been reported as 21% of the total electrical machine faults [23]. Hence, the characteristics of the SC currents should be thoroughly investigated in order to mitigate adverse effects in an EPS system. Results show that the peak value of the SC current is much higher than the rated current, being 6.9 times higher than rated in the SPM and 3.2 times higher in the IPM, as shown in Fig. 11.
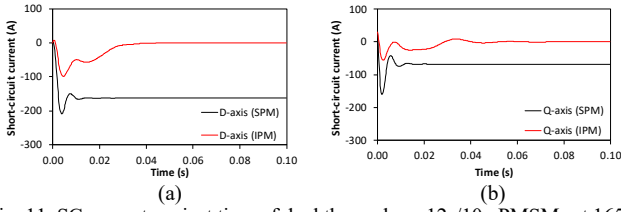
Fig. 11. SC current against time of dual three-phase 12s/10p PMSMs at 1650 rpm. (a) D-axis and (b) Q-axis currents.

The D-axis component in the SC current will not only become an issue for the power electronics devices but also can cause PM demagnetization. To investigate demagnetization, finite element analysis (FEA) has been carried out using N45SH as the permanent magnet material, which has the demagnetization knee point of 0.3 T at 150°C. FEA plots of magnet regions in both motors are shown in Fig. 12, for a peak D-axis current of 250 A. It shows that a portion of the magnet has a flux density magnitude of below 0.3 T and the magnet demagnetization ratio is 0.028 in the SPM. On other hand, the magnet demagnetization ratio in the IPM is circa zero, which indicates that there is no magnet region which has been permanently demagnetised. Therefore, the IPM topology has been chosen for further investigation, as detailed in section IV, based on its capability in limiting the SC current.
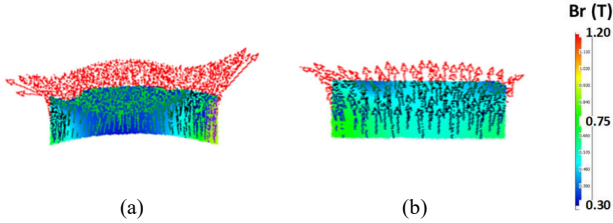

Fig. 12. Permanent magnet flux density and equal potential vector distribution for I_d = -250 A at 150°C PM in (a) SPM and (b) IPM motor.

IV. PERFORMANCE ENHANCEMENT OF IPMs FOR FAULT-TOLERANT EPS SYSTEM

A dual three-phase 12s/10p IPM motor with single layer winding is shown in Fig. 13(a), which only has one coil side in one stator slot. This type of winding layout is commonly adopted in the safety-critical applications, giving the benefit in physical, electromagnetic and thermal separation between phases [20]. Converting the winding layout from double layer to single layer which halves the number of phase vectors as shown in Fig. 13(b). It has been found that an IPM with single layer winding has minimal mutual coupling between phases, which is a great advantage for containing a fault locally without influencing other phases in the event of a fault. This phenomenon can also be seen from the inductance profile shown in Fig. 14.
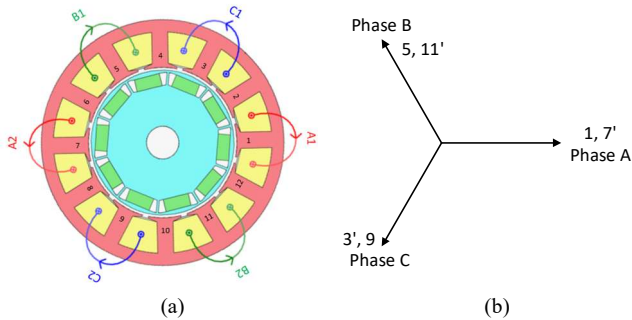

Fig. 13. Dual three-phase 12s/10p IPM with single layer winding. (a) Winding arrangement and (b) Phase vectors.
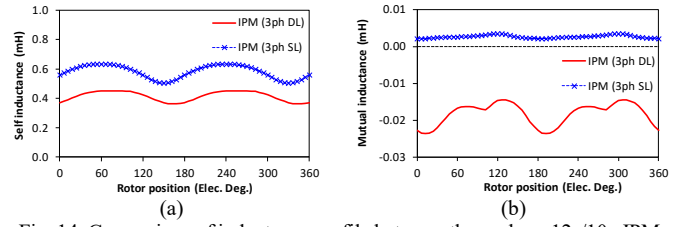

Fig. 14. Comparison of inductance profile between three-phase 12s/10p IPMs with double and single layer winding. (a) Self- and (b) Mutual-inductance.

It is found that an IPM with single layer winding has higher self-inductance L_{self} but negligible mutual inductance L_{mutual} compared to the double layer winding. Consequently, the steady state SC current I_{sc} can be characterized as [24].

$$I_{sc} = \frac{E_0}{\omega L_d} \qquad (1)$$

where E_0, ω and L_d are the open-circuit back-EMF, the stator supply angular frequency and D-axis inductance, respectively. Since the performance of the IPMs are investigated with the same magneto-motive force (MMF) and rotor speed, the increase of the inductance value in the single layer winding effectively limits the SC current (33% lower) and braking torque (55.2% lower) compared to double layer winding as shown in Fig. 15.
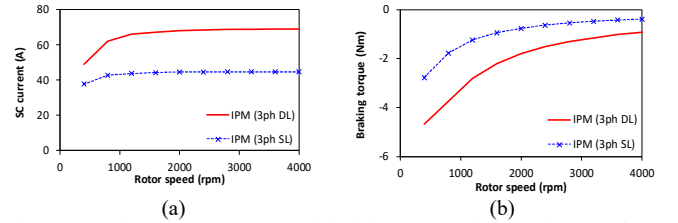

Fig. 15. Steady state SC current and braking torque of three-phase 12s/10p IPMs with double and single layer winding under a SC fault. (a) SC current under different speed and (b) Braking torque under different rotor speed.

A dual three-phase 12s/10p IPM with single layer winding Fig. 16(a) alongside the phase vectors shown in Fig. 16(b). The phase currents in two sets of windings have a 60 electrical degree phase shift as shown in Fig. 17, which is consistent with the phase shift in winding arrangement. Fig. 18(a) shows that dual three-phase IPM motor design can provide 5.75 N·m assisting torque under healthy operation. The spectrum in Fig. 18(b) shows that 6th harmonic is dominant while other harmonics are negligible. In the failure state of the motor, 50% of the assisting torque can be retained thanks to the remaining three-phase winding. Since the EPS motor is not always required to be active during driving, half of the rated motor torque is sufficient to allow the vehicle to be stopped safely.

In a conventional single three-phase PMSM, the winding failure directly leads to the complete performance loss, as depicted in Fig. 19.
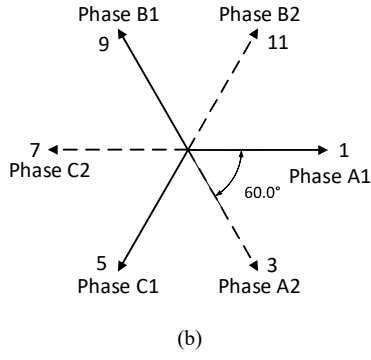

(a)

(b)
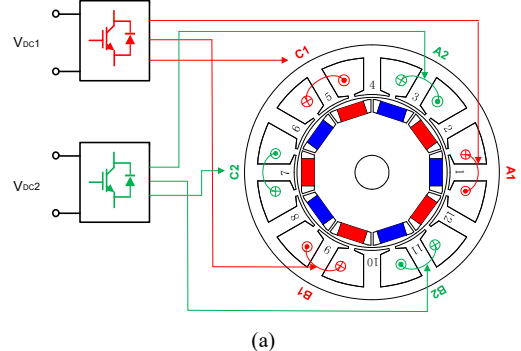
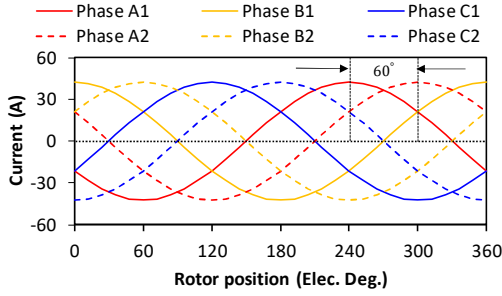Fig. 16. Dual three-phase 12s/10p IPM with single layer winding. (a) Winding arrangement and (b) Phase vectors.

Fig. 17. Phase current of dual three-phase winding for dual three-phase IPM.

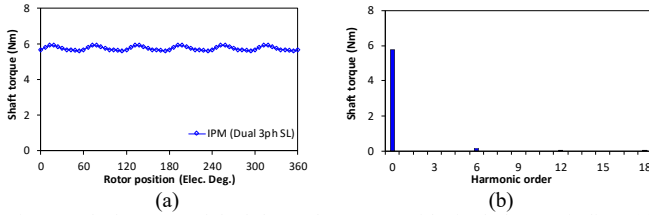(a)   (b)

Fig. 18. Shaft torque of dual three-phase IPM with single layer winding. (a) Waveforms and (b) Spectrum.
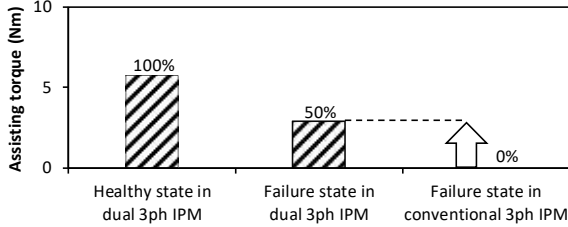

Fig. 19. Assisting torque state in three-phase and dual three-phase IPMs.

Any EPS motor requires low torque ripple in order to ensure smooth steering feel and decent noise, vibration and harshness (NVH) performance for the whole chassis system, although the requirement is somewhat relaxed in a SbW system because of the absence of direct coupling to the steering wheel [6], [21]. Hence, three-step skewing was applied to the rotor in order to reduce torque ripple, as illustrated in Fig. 20.

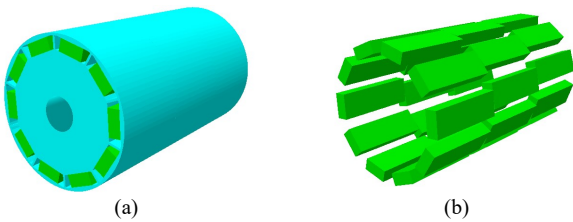(a)   (b)

Fig. 20. 3D view of three-step skewed IPM rotor. (a) Rotor and (b) Three-step skewed PM segments.

The optimal mechanical skewing angle was investigated and is found that the minimum torque ripple is 2.6% by step skewing with the skew angle of 8 mechanical degree albeit with some reduction in shaft torque as depicted in Fig. 21. The optimal skewing angle for the investigated IPM design was selected as 6 mechanical degree as a compromise between torque ripple reduction and torque capability.
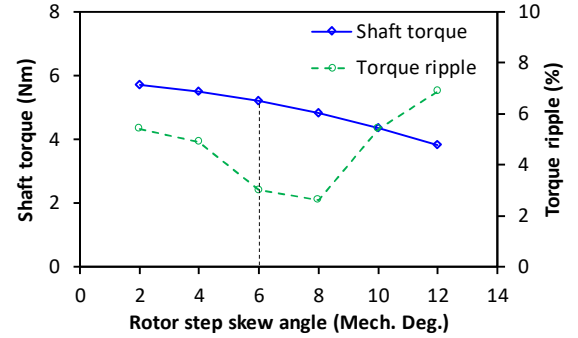

Fig. 21. Influence of rotor step angle against shaft torque and torque ripple.

In majority of cases, a large torque is only demanded from an EPS motor for parking or vehicle stopping. However, overload torque capability is important for some situations, which draw large current from inverter, such as 'lock-to-lock' steering operation. The overload capability of the IPM motor was investigated while factoring shaft torque and torque ripple as a function of RMS phase current as illustrated in Fig. 22. It is worth noting that duration of the operation is very important for PMSMs since high current for a long operation can end up with irreversible demagnetization for the magnets through excessive temperature rise. Samarium cobalt magnets could be adopted to increase thermal endurance of the EPS motor due to their superior temperature stability.
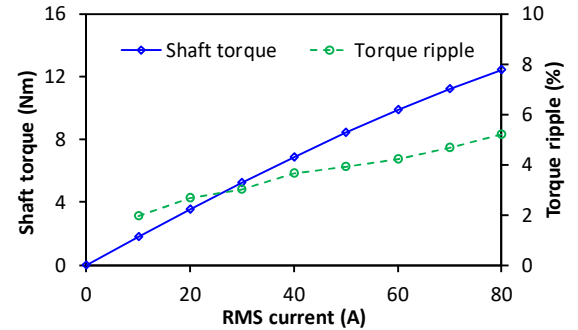
Fig. 22. Shaft torque and torque ripple against different RMS current.

V. CONCLUSION

This paper has reviewed the evolution process of different power steering systems to provide the background understanding issues in selecting an EPS motor. The observed merits and contributions of this paper can be summarised in the following main aspects:

- The IPM motor topology was chosen principally as it can limit short circuit current to an acceptable level. By converting the winding layout to single layer winding, the selected motor localizes the effect of a winding due to the reduced mutual coupling.

- Dual three-phase winding increases the system reliability and ensures the fail-operational capability for more advanced levels of autonomous vehicles. Step skewing is applied in the rotor side to mitigate torque ripple and ensure a smooth steering feel.

- The design procedure of an EPS system not only includes the design of the assisting motor but also the power electronics and mechanical design. The EPS motor should be further optimised as part of a system. However, the electromagnetic design procedure of the EPS motor in this paper serves as a practical procedure for selecting a motor topology for a specific vehicle type.

The experimental verification including failure mode and effect analysis, and control will be published in our future research.

REFERENCES

[1] M. Harrer and P. Pfeffer, "Steering handbook," *Springer*, London, 2017.

[2] D. J. Holt, "Electric steering: a revolution in steering technology," *Warrendale: Society of Automotive Engineers*, Vol. 58, Dec. 2001.

[3] D. Popa, A. Pop, C. Martiș and I. Vintiloiu, "Design of induction motor for electric power-assisted steering systems," *XXII International Conference. on Electrical Machines*, Lausanne, 2016, pp. 1566-1571.

[4] A. Matyas, G. Aroquiadassou, C. Martis, A. Mpanda-Mabwe and K. Biro, "Design of six-phase synchronous and induction machines for EPS," *The XIX International Conference on Electrical Machines*, Rome, 2010, pp. 1-6.

[5] C. Wang, J. Shen, P. Luk, W. Fei and M. Jin, "Design issues of an IPM motor for EPS," *COMPEL - The international journal for computation and mathematics in electrical and electronic engineering*, vol. 31, no. 1, 2012, pp. 71-87.

[6] J. Kim, M. Yoon, J. Hong and S. Kim, "Analysis of cogging torque caused by manufacturing tolerances of surface-mounted permanent magnet synchronous motor for electric power steering," *IET Electric Power Applications*, vol. 10, no. 8, pp. 691-696, 2016.

[7] K. Wang, Z. Q. Zhu, G. Ombach and W. Chlebosz, "Torque ripple and magnetic forces on teeth in IPM machines," *COMPEL - The international journal for computation and mathematics in electrical and electronic engineering*, vol. 33, no. 5, 2014, pp. 1487-1501.

[8] P. Andrada, B. Blanque, E. Martinez, J. I. Perat, J. A. Sanchez and M. Torrent, "Switched reluctance motor for electric power-assisted steering," *13th European Conference on Power Electronics and Applications*, Barcelona, 2009, pp. 1-9.

[9] J. Ahn, S. Lim, K. Kim, J. Lee, J. Choi, S. Kim and J. Hong, "Field weakening control of synchronous reluctance motor for electric power steering," *IET Electric Power Applications*, vol. 1, no. 4, pp. 565-570, July 2007.

[10] M. Hiramine, Y. Hayashi, and T. Suzuki, "2-drive motor control unit for electric power steering," *SAE International Journal Passenger Cars – Electron. Electrical System.* Vol. 10, no. 2, pp. 337-344, 2017.

[11] J. Hayashi, "Road map of the motor for an electrical power steering system," *Chassis Tech plus 4th International Munich Chassis Symposium*, pp. 317-326, 2013.

[12] M. Barcaro, N. Bianchi and F. Magnussen, "Analysis and tests of a dual three-phase 12-slot 10-pole permanent-magnet motor," *IEEE Transactions on Industrial. Applications,* vol. 46, no. 6, pp. 2355-2362, Nov.-Dec. 2010.

[13] C. Martis, C. Oprea, I. Viorel and J. Gyselinck, "Design of a fault-tolerant 6-phase switched reluctance motor for electric power-assisted steering systems," *IEEE International Electrical Machines and Drives Conference, Miami*, FL, 2009, pp. 993-998.

[14] T. Nakayama and E. Suda. "The present and future of electric power steering." *International Journal of Vehicle Design*, vol. 15, no. 3-5, pp. 243-254, 1994.

[15] C. Becker, A. Nasser, F. Attioui, D. Arthur, A. Moy and J. Breweret, "Functional safety assessment of a generic electric power steering system with active steering and four-wheel steering features," *United States. Department of Transportation. National Highway Traffic Safety Administration, Tech. Rep.*, 2018.

[16] C. Huang, F. Naghdy, H. Du, and H. Huang, "Fault tolerant steer-by-wire systems: An overview," *Annual Reviews in Control*, vol. 47, pp. 98–111, 2019.

[17] M. Würges, "New electrical power steering systems," *Encyclopedia of Automotive Engineering*, pp. 1-17, April, 2014.

[18] S. A. Mortazavizadeh, A. Ghaderi, M. Ebrahimi and M. Hajian, "Recent developments in the vehicle steer-by-wire system," *IEEE Transactions on Transportation Electrification*, vol. *6, no.* 3, pp. 1226-1235, 2020.

[19] V. Chahare, I. Mhaisne, and D. Dongre, "An overview on future electricsteering system: A project approach," *International Research Journal of Engineering and Technology*, vol. 4, no. 7, pp. 2152–2159, 2017.

[20] D. Ishak, Z. Q. Zhu and D. Howe, "Comparison of PM brushless motors, having either all teeth or alternate teeth wound," *IEEE Transactions on Energy Conversion*, vol. 21, no. 1, pp. 95-103, March, 2006.

[21] X. Ge, Z. Q. Zhu, G. Kemp, D. Moule and C. Williams, "Optimal step-skew methods for cogging torque reduction accounting for three-dimensional effect of interior permanent magnet machines," *IEEE Transactions on Energy Conversion*, vol. 32, no. 1, pp. 222-232, March 2017.

[22] H. Yang, S. Ademi and R. McMahon, "Comparative study on multiple three-phase permanent magnet motors in fault tolerant electric power steering application," *10th International Conference on Power Electronics, Machines and Drives*, Nottingham, UK, Dec. 2020.

[23] A. H. Bonnett and C. Yung, "Increased efficiency versus increased reliability," *IEEE Industrial Application Magazine*, vol. 14, no. 1, pp. 29–36, Jan./Feb. 2008.

[24] N. Mohan, T. M. Undeland, and W. P. Robbins, "Power Electronics: Converters," *Applications, and Design.* John Wiley & Sons, Inc. 2003, pp. 485-487.

Han Yang received the B.Eng both from Nanjing Normal University and University of Northumbria at Newcastle in 2013, the M.Sc. degree at the University of Sheffield in 2014, and the Ph.D. degree at the University of Sheffield in 2019, all in Electronic and Electrical Engineering. He is currently working as a Research Fellow in Warwick Manufacturing Group, University of Warwick, U.K.. His research interest include design and analysis of fault-tolerant permanent magnet motors for vehicle applications.

Sul Ademi received the B.Eng. and Ph.D. degrees in electrical and electronics engineering from Northumbria University, Newcastle upon Tyne, U.K., in 2011 and 2014, respectively. From 2015 to 2017, he was a Lead Researcher, engaged in knowledge exchange and transfer partnership activities between University of Strathclyde, Glasgow, U.K. and GE Grid Solutions, Stafford, U.K. He is currently a Research Scientist with the Warwick Manufacturing Group, University of Warwick, Coventry, U.K. His research interests include electric motor drives, control of doubly-fed machines, and design and analysis of novel permanent-magnet machines.

Jesús Paredes received the M.Sc. degree in industrial engineering from the University of Navarra, San Sebastian, Spain, in 2016. He was with Cetest, Beasain, Spain, where he worked in railway systems radiated emission tests, in 2015. He is currently a Researcher with the CEIT, Donostia-San Sebastian, Spain, and collaborates with the University of Navarra as a Lecturer Assistant. His research activity focuses on design of high-power density electric machines. He is the coauthor of publications regarding the more electric aircraft and synchronous reluctances machines.

Richard McMahon received the B A. degree in electrical sciences and the Ph D. degree from the University of Cambridge, Cambridge, U.K., in 1976 and 1980, respectively. Following postdoctoral work on semiconductor device processing, he became a University Lecturer in electrical engineering in 1989 with the Engineering Department, University of Cambridge, where he was a Senior Lecturer in 2000. In 2016, he was with the Warwick Manufacturing Group, University of Warwick, Coventry, U.K., as a Professor of power electronics. His current research interests include electrical drives, power electronics, and semiconductor materials.